

## Neuroimaging

Resting-state network dysfunction in Alzheimer's disease:  
A systematic review and meta-analysisAmanPreet Badhwar<sup>a,b,\*</sup>, Angela Tam<sup>a,c,d</sup>, Christian Dansereau<sup>a,b</sup>, Pierre Orban<sup>a,b,d</sup>,  
Felix Hoffstaedter<sup>e,f,g</sup>, Pierre Bellec<sup>a,b,\*\*</sup><sup>a</sup>Centre de Recherche, Institut Universitaire de Gériatrie de Montréal, Montreal, Quebec, Canada<sup>b</sup>Université de Montréal, Montreal, Quebec, Canada<sup>c</sup>McGill University, Montreal, Quebec, Canada<sup>d</sup>Douglas Mental Health University Institute Research Centre, Montreal, Quebec, Canada<sup>e</sup>Institute of Neuroscience and Medicine (INM-1, INM-7), Research Centre Jülich, Jülich, Germany<sup>f</sup>Institute of Clinical Neuroscience and Medical Psychology, Heinrich Heine University Düsseldorf, Düsseldorf, Germany<sup>g</sup>Institute of Systems Neuroscience, Heinrich Heine University Düsseldorf, Düsseldorf, Germany

## Abstract

**Introduction:** We performed a systematic review and meta-analysis of the Alzheimer's disease (AD) literature to examine consistency of functional connectivity alterations in AD dementia and mild cognitive impairment, using resting-state functional magnetic resonance imaging.**Methods:** Studies were screened using a standardized procedure. Multiresolution statistics were performed to assess the spatial consistency of findings across studies.**Results:** Thirty-four studies were included (1363 participants, average 40 per study). Consistent alterations in connectivity were found in the default mode, salience, and limbic networks in patients with AD dementia, mild cognitive impairment, or in both groups. We also identified a strong tendency in the literature toward specific examination of the default mode network.**Discussion:** Convergent evidence across the literature supports the use of resting-state connectivity as a biomarker of AD. The locations of consistent alterations suggest that highly connected hub regions in the brain might be an early target of AD.© 2017 The Authors. Published by Elsevier Inc. on behalf of the Alzheimer's Association. This is an open access article under the CC BY-NC-ND license (<http://creativecommons.org/licenses/by-nc-nd/4.0/>).

## Keywords:

Resting-state fMRI; Functional connectivity; Alzheimer's disease; Mild cognitive impairment; Meta-analysis

## 1. Introduction

Alzheimer's disease (AD) exists on a continuum comprising a lengthy preclinical stage, a middle stage of mild cognitive impairment (MCI), and a final stage of dementia [1]. Symptoms usually start around the age of 65

years, except in rare patients with early onset (33–60 years) autosomal dominant AD (ADAD) [2,3]. Drugs currently available for AD provide limited short-term treatment of AD symptoms [4]. Trials of disease-modifying therapies for AD dementia patients have been unsuccessful, likely because intervention at this stage is too late to affect the neurodegenerative process. The focus now is on therapeutic intervention at the MCI and/or preclinical disease stages, with delay of dementia onset constituting a major clinical end point for clinical trials [1]. This approach depends on the identification of biomarkers that can aid early AD diagnosis [1,5]. Currently, validated AD biomarkers are (1) low cerebrospinal fluid (CSF) amyloid- $\beta$  42 levels and/or high

---

\*Corresponding author. Tel.: +1-514-340-3540x3367; Fax: +1-514-340-2802.

\*\*Corresponding author. Tel.: +1-514-340-3540x4782; Fax: +1-514-340-2802.

E-mail address: [amanpreet.badhwar@criugm.qc.ca](mailto:amanpreet.badhwar@criugm.qc.ca) (A.B.), [pierre.bellec@criugm.qc.ca](mailto:pierre.bellec@criugm.qc.ca) (P.B.)

amyloid tracer retention on positron emission tomography (PET), indicating brain amyloidosis; (2) high CSF tau levels, indicating neuronal injury; (3) temporoparietal pattern of reduced 18F-fluorodeoxyglucose uptake on PET, indicating brain hypometabolism, and (4) patterns of brain atrophy on structural magnetic resonance imaging (MRI), indicating neurodegeneration [1,6].

Connectivity in resting-state functional magnetic resonance imaging (rsfMRI) is an emerging AD biomarker that holds promise for early diagnosis [1,5,7]. RsfMRI indirectly measures neural processing in the brain using blood oxygenation and can be used to identify spatially distributed networks [8]. The National Institute on Aging–Alzheimer's Association lists rsfMRI functional connectivity as a potential biomarker of neuronal injury, at an early stage of validation [6]. The existing literature is indeed mostly composed of proof-of-concept cross-sectional comparisons of cognitively healthy elderly individuals with patients suffering from mild (MCI) or severe (dementia) AD symptoms.

To date, multiple studies have reported intrinsic connectivity network (ICN) disturbances in patients with AD dementia and MCI, presymptomatic ADAD mutation carriers, and cognitively normal individuals carrying the at-risk APOEε4 allele and/or showing evidence of amyloidosis [9–12]. Despite such promising findings, the overall effect of AD on ICNs remains poorly characterized because of several inconsistencies in the literature, such as different acquisition protocols, processing methods, and/or exclusion/inclusion criteria [13]. Our aim was to perform a systematic review and meta-analysis to examine the consistency of intrinsic connectivity alterations in MCI and late-onset AD (LOAD) dementia across the literature. We also reviewed the burgeoning literature on connectivity abnormalities in ADAD and the at-risk APOEε4 genotype.

## 2. Methods

### 2.1. Literature search

We conducted a systematic review of PubMed articles up to December 3, 2015 in accordance with the Preferred Reporting Items for Systematic Reviews and Meta-Analyses guidelines [14]. Search terms and combinations used are provided in [Supplementary Table 1](#). Results were filtered for duplicates within each of the two main search categories, that is, AD dementia or MCI patients ([Fig. 1](#)). Unique search results underwent further screening as described subsequently.

### 2.2. Study selection

Search results were subjected to two successive screenings with increasingly stringent criteria. The initial screen was performed on article abstracts. An article was included if the abstract indicated that it was a peer-reviewed original research article written in English and used rsfMRI to study

LOAD and/or MCI in humans. Reviews, letters, case reports, and studies with subjects in whom MCI was associated with other diseases were omitted. Following the initial screening, we applied the following inclusion criteria: (1) used seed-based or independent component analysis rsfMRI methods; (2) investigated functional connectivity between patients (AD dementia or MCI) and age-matched healthy controls (HC); and (3) reported peak coordinates of significant statistical differences in average connectivity between groups and the direction of difference.

### 2.3. Data extraction

One reviewer (A.B.) conducted the searches and screened for duplicates. Two reviewers (A.B. and A.T.) independently screened all unique search results for potential inclusion in the meta-analysis. Only articles passing both reviewers' approval were considered for final inclusion. For each “included” article, coordinate data of significant between-group comparisons, such as AD versus HC, were transcribed by one reviewer and checked by two others (second reviewer [A.T.] and F.H.).

### 2.4. Meta-analysis

We performed complementary network- and voxel-based quantitative meta-analyses on six main group comparisons: pooled group with AD dementia and MCI patients termed ADMCI < HC, ADMCI > HC, MCI < HC, MCI > HC, AD < HC, and AD > HC. Although the voxel-based meta-analysis has finer spatial resolution for findings with high anatomic consistency, we assumed the network-based approach would have better sensitivity for detecting consistent involvement of anatomically distributed networks. Coordinates from articles using the same cohort were pooled under the PubMed unique identifier or PMID of the earliest publication and treated as results from a single study to avoid counting the cohort multiple times. Henceforth, an individual article will be referred to as a “study” and a group comparison yielding network and/or localization information (e.g., ADMCI < HC) as a “contrast.”

#### 2.4.1. Network-based statistics

We performed network-based statistics on seed coordinates (seed statistics) to assess whether seed regions were preferentially selected from within certain networks in the literature. We also performed network-based statistics on coordinate data of significant contrasts (contrast statistics) to assess the consistency of network-level findings in the AD literature. In particular, we performed three types of contrast statistics: (1) all coordinates irrespective of seed network; and given the focus on the default mode network (DMN) in the literature, (2) coordinates associated with seeds inside the DMN only; and (3) coordinates associated with seeds outside the DMN, that is, non-DMN seeds. All analyses were conducted using a multiresolution atlas of group-level

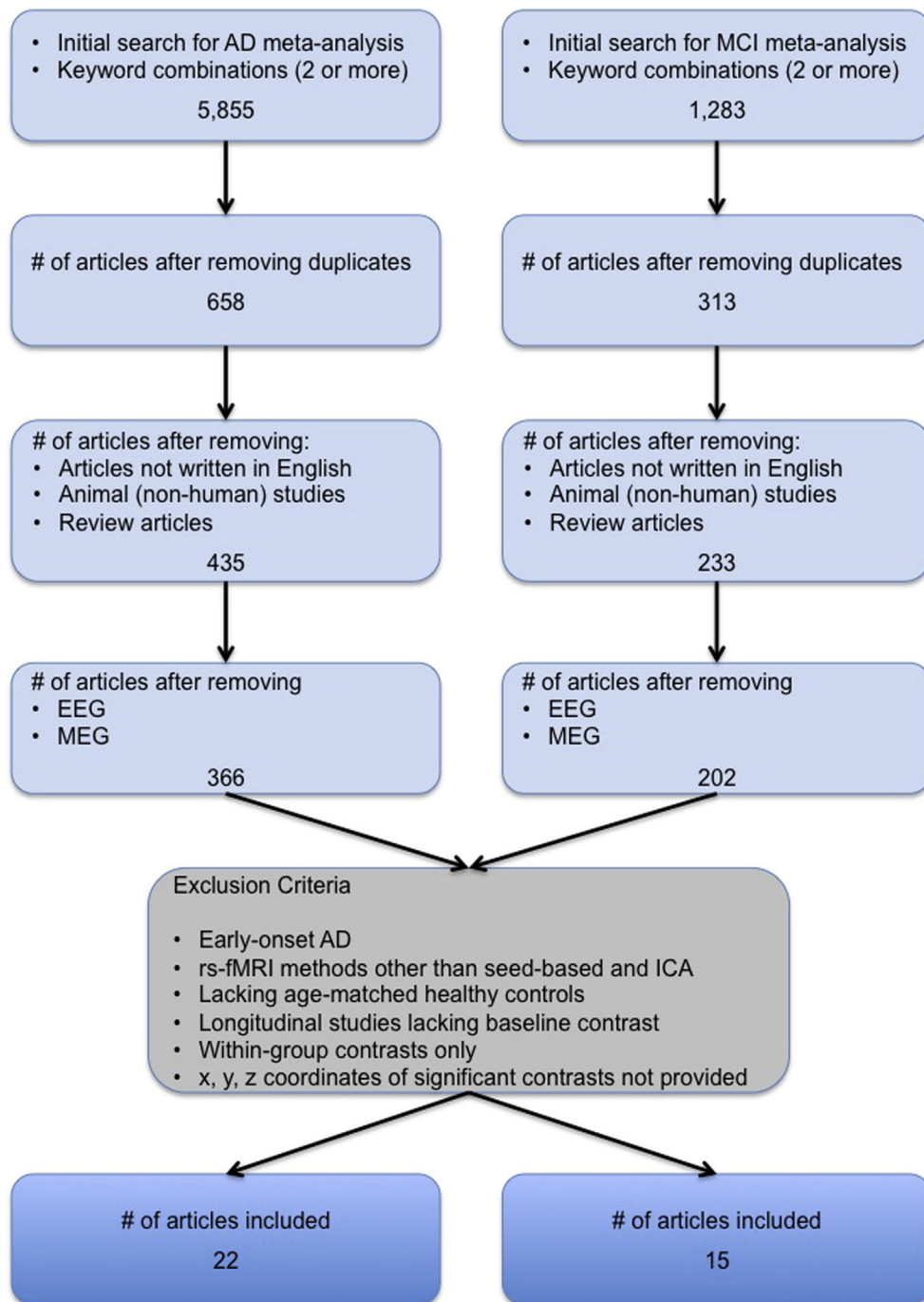


Fig. 1. Flowchart of the study selection process. Selection process for AD and MCI studies included in the meta-analyses. Studies using rsfMRI methods dissimilar to seed-based and ICA methods, such as degree centrality or graph theory, amplitude of low-frequency fluctuations, and regional homogeneity were not included. Abbreviations: AD, Alzheimer's disease; EEG, electroencephalogram; ICA, independent component analysis; MCI, mild cognitive impairment; MEG, magnetoencephalography; rsfMRI, resting-state functional magnetic resonance imaging.

functional brain parcellations derived from an independent rsfMRI data set, the Bootstrap Analysis of Stable Clusters–Cambridge atlas (<https://dx.doi.org/10.6084/m9.figshare.1285615.v1>) [15]. This atlas consists of nine functional parcellations capturing successively finer levels of spatial detail, of which we used parcellations at two resolutions: the first comprised seven commonly used large-scale networks

(R7 atlas) and the second containing 36 networks (R36 atlas). We used R7 and R36 atlases for contrast statistics and only the R7 atlas for seed statistics. Because seeds were assigned indirectly for studies where coordinates were not provided, indirect assignment could not be performed with sufficient precision to use the R36 atlas. Assignment of seeds to one of the R7 networks was based on published coordinates,

when available. When only anatomic labels were provided for seed regions, network assignment was based on (1) the center of gravity in MNI space or (2) visual approximation if no further information was available. For independent component analysis-based studies, network assignment was based on (1) network coordinates when provided or (2) visual assignment to one or more of the seven networks based on the degree of spatial overlap.

We tested the spatial consistency of both seed and peak locations using the following approach. For each study, we computed the number of coordinates falling within each network, after conversion of Talairach space coordinates into MNI space using the Lancaster transform [16], when necessary. Coordinates falling outside of the gray matter mask (ICBM152) were assigned to the closest network. To remain unbiased to the number of coordinates reported per study, we computed the ratio of coordinates falling within each network to the total number of coordinates reported per study. This ratio was then averaged across studies. The significance of findings was assessed using Monte Carlo permutation tests. Using the total number of coordinates per study, we generated a random assignment of coordinates to networks, taking into consideration the volume of each network. Coordinate counts per network were normalized as described previously, followed by an averaging across studies. This Monte Carlo sampling process was repeated 10,000 times. Thereafter, we compared the distribution of the average frequency obtained from the random sampling with the frequency obtained from the meta-analysis, resulting in  $P$  value estimates [17]. Multiple comparisons across networks were accounted for using a false discovery rate (FDR) procedure (qFDR < 0.05) [18]. The  $P$  values less than .05 that did not survive multiple comparisons were deemed as “trends.”

#### 2.4.2. Voxel-based statistics

Voxel-level statistical analysis was performed using activation likelihood estimation (ALE), a widely used algorithm for coordinate-based meta-analysis of neuroimaging studies. ALE aims at delineating brain regions with above-chance convergence of reported coordinates across experiments [19]. Coordinates falling outside the gray matter mask were removed from the analysis. We used the in-house ALE algorithm implementation in MATLAB version 8.3.0.532, which treats each of the coordinates in a given experiment as a three-dimensional gaussian probability distribution centered at the given coordinate. The probability distributions acknowledge the spatial uncertainty associated with each experiment. For any given study, the width of the spatial uncertainty of its coordinates is determined based on empirical data on the between-subject and between-template variances representing the main components of this uncertainty [19]. Then, the probability distributions of all coordinates per included study are combined for each voxel, generating a modeled activation (MA) map. To limit the effect of multiple coordinates very close to one another within a given study, we used the “nonadditive” approach,

which calculates MA maps by taking the maximum probability across overlapping gaussians [19]. ALE scores were computed on a voxel-by-voxel basis by taking the union across these MA maps. To distinguish between “true” and random convergence between studies (i.e., noise), ALE scores were compared with a null distribution reflecting a random spatial association between experiments (10,000 permutations). Nonparametric  $P$  values were assessed at a familywise error-corrected threshold of  $P < .05$  on a cluster level (cluster-forming threshold:  $P < .001$  at voxel level) and transformed into  $t$  scores for display purposes. Only contrasts including more than 18 experiments were considered, as recommended in a recent large-scale simulation study [20].

### 3. Results

#### 3.1. Search results

The results of the initial search, along with studies systematically excluded from inclusion in our rsfMRI meta-analyses are presented in Fig. 1. Thirty-four studies totaling 1363 subjects (post pooling of identical cohorts) met our inclusion criteria and were included in the meta-analysis. The total included 352 MCI, 378 AD dementia (specifically LOAD), and 633 HC. Diagnostic criteria used per study for MCI and AD dementia are provided in the [Supplementary Material \(Supplementary Table 2 and Section 2\)](#). The bulk (54%) of the studies had 20 or less subjects per group. Twenty studies (66.7%) investigated rsfMRI connectivity measures with other domains, cognition being most frequent ( $n = 11/22$  AD studies,  $n = 9/15$  MCI studies), and few with levels of amyloid burden using Pittsburgh compound B ( $n = 3$ ), brain atrophy ( $n = 3$ ), and structural connectivity ( $n = 1$ ). Alterations in functional connectivity were often ( $n = 5/9$  studies) reported to be significantly correlated with episodic verbal learning and memory in MCI cohorts. [Table 1](#) provides additional characteristics of the included rsfMRI studies, including scanner make, model, and strength, and seed region and/or ICN investigated. A summary of commonly used preprocessing steps utilized by the studies present in our meta-analysis are provided in [Supplementary Table 3](#).

#### 3.2. Network-based meta-analysis

##### 3.2.1. Seed statistics

Using network-level statistics, we demonstrated that a disproportionately large number of studies specifically targeted the DMN ([Fig. 2](#)) irrespective of the population (ADMCI, MCI, or AD dementia) being studied.

##### 3.2.2. Contrast statistics

We first examined R7 network-level statistics and all seeds combined. Aberrant functional brain connectivity was observed in ADMCI, MCI, and AD, relative to HC ([Fig. 3](#)). In the ADMCI cohort, we found both significant

Table 1  
Characteristics of rsfMRI studies included in the meta-analysis

Study	N	AD					HC					AD		Scanner	Method	Seed region/ICN investigated
		n	M	F	Age	SD	n	M	F	Age	SD	<HC	>HC			
Wang et al. [63]	28	14	7	7	70.2	6.3	14	7	7	69.6	5.5	x		1.5 T S	SB	PCC
Zhang et al. [64] <sup>a</sup>	32	16	6	10	71.6	5.1	16	7	9	71.3	4.9	x	x	1.5 T P	SB	PCC
Zhang et al. [65] <sup>a</sup>	55	39	18	21	73.4		16	7	9	71.3	4.9	x	x	1.5 T P	SB	PCC
Sheline et al. [66]	83	35					48					x	x	3.0 T S	SB	Precuneus
Zhou et al. [52]	24	12	5	7	63.3	7.7	12	5	7	62.0		x	x	1.5/3.0/4.0 T S/GE/B	SB and ICA	AG (l), pregenual ACC (r)
Gili et al. [67] <sup>*</sup>	21	11	7	4	71.9	7.9	10	7	3	64.1	10.5	x		3.0 T S	SB and ICA	PCC, mPFC
Wu et al. [68] <sup>b</sup>	31	15	6	9	64.0	8.3	16	7	9	65.0	9.2	x		3.0 T S	ICA	DMN
Li et al. [69] <sup>b</sup>	31	15	6	9	64.0	8.3	16	7	9	65.0	9.2	x		3.0 T S	ICA	ATN (d, v)
Damoiseaux et al. [70]	39	21	9	12	64.2	8.7	18	12	6	62.7	10.3	x	x	3.0 T GE	ICA	DMN (a, p, v), SMN
Binnewijzend et al. [71] <sup>†</sup>	82	39	23	16	67.0	8.0	43	23	20	69.0	7.0	x		1.5 T S	ICA	DMN, working memory (l, r), visuospatial attention (d), spatial attention (v), SMN, auditory language, prVIS, sVIS, basal ganglia cerebellum
Kenny et al. [72]	32	16			77.3	8.9	16			76.3	8.3		x	3.0 T P	SB	Hippocampus (l, r), PCC, precuneus, prVIS
Zhu et al. [73] <sup>†</sup>	22	10	7	3	72.9	7.9	12	5	7	73.8	6.5	x		3.0 T GE	SB	ICC (l, r)
Balthazar et al. [74]	37	20			73.9	8.2	17			72.3	6.4	x	x	3.0 T P	ICA	DMN (d, v), SN (a, p)
Yao et al. [75] <sup>c,†</sup>	62	35	12	23	72.4	8.5	27	16	11	69.2	6.5	x		3.0 T GE	SB	Amygdala (l, r)
Zhou et al. [76] <sup>c,†</sup>	62	35	12	23	72.4	8.5	27	16	11	69.2	6.5	x	x	3.0 T GE	SB	T
Zhang et al. [77] <sup>c,†</sup>	62	35	12	23	72.4	8.5	27	16	11	69.2	6.5	x		3.0 T GE	SB	MrD (l, r)
Gour et al. [29]	28	14	6	8	75.1	2.9	14	4	10	72.8	3.0	x	x	3.0 T S	SB	PCC, perirhinal cortex (l, r), dlPFC (l, r)
Weiler et al. [78]	48	22	6	16	73.4	5.7	26	6	20	70.0	6.6	x	x	3.0 T P	SB	PCC, Wernicke's (l); Broca's (l), dlPFC (l, r), saVC
Balachandar et al. [79]	30	15	9	6	67.3	6.6	15	9	6	64.4	8.9	x	x	3.0 T S	ICA	DMN, thalamic, ECN
Pasquini et al. [80] <sup>*</sup>	43	21	8	13	72.3	8.6	22	6	16	66.3	9.0	x	x	3.0 T P	ICA	DMN (a, p)
Adriaanse et al. [28]	59	28	17	11	72.0	4.9	31	17	14	72.0	4.3	x		1.5 T S	ICA	DMN, VIS (med, lat), AN, SMN, ECN, dorsovisual (l, r)
Yi et al. [81] <sup>*</sup>	23	11	1	10	64.2	2.4	12	3	9	71.8	1.2	x		3.0 T GE	ICA	DMN, SN

(Continued)

Table 1  
Characteristics of rsfMRI studies included in the meta-analysis (*Continued*)

Study	N	MCI					HC					MCI		Scanner	Method	Seed region/ICN investigated
		n	M	F	Age	SD	n	M	F	Age	SD	<HC	>HC			
Sorg et al. [82]	40	24	13	11	69.3	8.1	16	10	6	68.1	3.8	x		1.5 T S	ICA	VIS, AN, ATN (v), spatial attention, DMN
Bai et al. [83]	56	30	15	15	72.5	4.4	26	12	14	71.6	5.3	x	x	1.5 T GE	SB	PCC
Gili et al. [67]*	20	10	6	4	71.2	4.1	10	7	3	64.1	10.5	x		3.0 T S	<i>SB and ICA</i>	PCC, mPFC
Bai et al. [84]	44	26	19	7	71.4	4.3	18	10	8	70.3	4.7		x	1.5 T GE	ICA	DMN
Xie et al. [85]	56	30	19	11	72.6	4.8	26	14	12	70.3	4.8	x		1.5 T GE	SB	Postcentral gyrus (l), hippocampus (l), medialFC (l), middleFC (l), precuneus (l, r), insula (l, r)
Jin et al. [86]	16	8	5	3	60.6	3.2	8	4	4	60.9	8.3	x	x	3.0 T GE	ICA	DMN
Han et al. [87]	80	40	7	33	86.3	4.5	40	15	25	86.3	4.5	x	x	1.5 T GE	SB	PCC
Liang et al. [88]	32	16	6	10	68.5	7.8	16	6	10	67.2	8.4	x	x	3.0 T S	SB	AG (l, r), supramarginal gyrus (l, r), intraparietal sulcus (r)
Hahn et al. [89] <sup>†</sup>	54	28	14	14	69.5	7.1	26	10	16	65.5	7.8	x		3.0 T P	ICA	DMN (a, p), ATN (d, v), ECN (l, r), SMN, VIS
Myers et al. [90]	35	23	14	9	69.3	7.4	12	5	9	63.8	5.2	x		3.0 T P	ICA	DMN (a, p), ATN (l, r, d), SN, prAN
Koch et al. [91]	40	24	14	10	68.2	8.4	16	7	9	64.8	5.4	x		3.0 T P	ICA	DMN (a, p), ATN (l, r, d), SN, prAN
Pasquini et al. [80]*	44	22	11	11	65.3	8.7	22	6	16	66.3	9.0		x	3.0 T P	ICA	DMN (a, p)
Das et al. [92]	69	30	14	16	71.6	6.8	39	18	21	70.6	9.0	x		3.0 T S	SB	Hippocampal subregions
Gardini et al. [93]	42	21	13	8	70.6	4.7	21	7	14	69.8	6.5		x	3.0 T GE	SB	PCC, mPFC
Yi et al. [81]*	32	20	4	16	71.0		12	3	9	71.8	1.2	x	x	3.0 T GE	ICA	DMN, SN

Abbreviations: a, anterior; ACC, anterior cingulate cortex; AD, Alzheimer's disease; AG, angular gyrus; AN, auditory network; ATN, attentional network; B, Brucker; d, dorsal; dIPFC, dorsolateral prefrontal cortex; DMN, default mode network; ECN, executive control network; F, female; GE, General Electrics; HC, healthy control; ICA, independent component analysis; ICC, isthmus of cingulate cortex; ICN, intrinsic connectivity network; l, left; lat, lateral; M, male; MCI, mild cognitive impairment; med, medial; medialFC, medial frontal cortex; middleFC, middle frontal cortex; mPFC, medial prefrontal cortex; MrD, marginal division; n, number of subjects; p, posterior; P, Philips; PCC, posterior cingulate cortex; prAN, primary auditory network; prVIS, primary visual network; r, right; rsfMRI, resting-state functional magnetic resonance imaging; S, Siemens; saVC, secondary associative visual cortex; SB, seed based; SMN, sensorimotor network; SD, standard deviation; sVIS, secondary visual network; T, Tesla; v, ventral.

NOTE. Data provided in "bold" indicate seven studies using shared cohorts. Coordinates from these seven studies were subsequently pooled under four studies (indicated by superscript letters a, b, and c), under the corresponding earliest publication using the cohort. In column "Method", when both seed-based and ICA rsfMRI methods were used by a study, the method given in "italics" indicates the method associated with reported coordinates. For column "Seed region/ICN investigated", all seed regions and ICNs investigated are listed, irrespective of significant findings.

\*Studies reporting significant coordinates for both AD and MCI patients, relative to matched HC.

<sup>†</sup>Studies investigating both AD dementia and MCI cohorts.

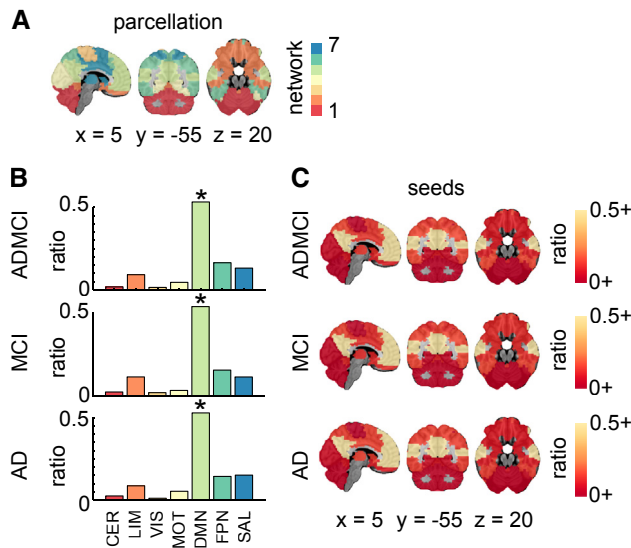


Fig. 2. Seed region network-level findings. (A) R7 atlas; (B) histograms showing the ratio of counts (or hits) across the seven networks for all seeds in ADMCI, MCI, and AD. Significant (\* denoting  $qFDR < 0.05$ ) prevalence of seeds in the DMN was demonstrated across all three cohorts; (C) seed region hit maps (ratio of dysconnectivity coordinates in each network) at R7. Maps are superimposed onto the anatomic International Consortium for Brain Mapping (ICBM) 152 template. x, y, and z Montreal Neurological Institute (MNI) coordinates are given for sagittal, coronal, and axial slices. Abbreviations: AD, Alzheimer's disease; ADMCI, AD dementia and MCI; CER, cerebellar network; DMN, default mode network; FDR, false discovery rate; FPN, frontoparietal network; HC, healthy control; LIM, limbic network; MCI, mild cognitive impairment; MOT, motor network; SAL, salience network; VIS, visual network.

hypoconnectivity and hyperconnectivity in the DMN. Significant hyperconnectivity in the DMN and limbic network (LIM) was observed in the MCI cohort. There was also significant hypoconnectivity in the DMN for the AD group, which appeared as a trend for the MCI group.

We then refined the spatial localization of effects found in R7 using the R36 atlas. Significant DMN hypoconnectivity in AD and ADMCI cohorts was detected in the precuneus (PCu) and posterior cingulate cortex (PCC) (Fig. 4). A trend for DMN hyperconnectivity was observed in the PCu for ADMCI and in both the PCu and PCC in MCI (Fig. 4). The LIM hyperconnectivity was observed as a trend in the hippocampus and entorhinal cortex in MCI patients (Fig. 4).

Finally, we investigated the robustness of findings with respect to the selection of seeds (DMN, non-DMN, or all combined), using the R7 atlas. Significant network-level findings derived from all seeds combined, as reported previously, replicated when using DMN seeds alone (Fig. 3A). In addition, a trend toward hypoconnectivity in MCI became significant using DMN seeds only. When focusing on non-DMN seed studies, no significant effects were observed in the DMN, as expected. The only significant result was hyperconnectivity of the salience network (SAL) in ADMCI, also present as a trend in AD subjects.

### 3.3. Voxel-based meta-analysis

ALE results demonstrated significant hypoconnectivity in the PCC and PCu in the ADMCI and AD studies (Fig. 5, Supplementary Table 4), consistent with our network-level findings using R7 and R36 atlases. This observation was made both for all seeds combined and DMN-only seeds (Fig. 5, Supplementary Table 4).

Unlike the network-level analysis, using ALE we found diminished connectivity in the primary visual cortex, both in ADMCI and AD. This was observed for all seeds combined as well as for DMN-only seeds in ADMCI and DMN-only seeds in AD. Finally, significant hyperconnectivity was observed in AD in the anterior insula (Fig. 5, Supplementary Table 4), consistent with the trend in the LIM observed using the R36 atlas.

## 4. Discussion

We report on a systematic meta-analysis of rsfMRI brain connectivity dysfunction in LOAD, using voxel-, region-, and network-level statistics. Our results demonstrated consistent connectivity alterations both within and outside of the DMN.

### 4.1. Connectivity changes in the DMN

#### 4.1.1. Late-onset AD

Our results revealed a consistent decrease in DMN connectivity in the ADMCI and AD cohorts, particularly in the PCu and PCC, for all resolutions of meta-analysis. This finding is in line with previous meta-analyses centered on the DMN [21,22], and a recent study published after we completed our analysis [23]. DMN deterioration appears robust to the choice of analytical approaches, as previous meta-analyses largely included studies measuring regional homogeneity and amplitude of low-frequency fluctuation. Moreover, our results support previous literature reporting on the vulnerability of the DMN to multiple AD pathophysiology [24].

Unlike our robust findings in AD subjects, DMN hypoconnectivity in MCI could only be demonstrated using network-level statistics, suggesting a weaker, more distributed effect in MCI. However, we recently reported decreased DMN connectivity in a large multisite MCI cohort with a connectome-wide approach [13]. The modest findings of our present meta-analysis may be because of a lack of statistical power from having multiple, small, single-site samples. Clinical heterogeneity might also have played a role, that is, only a subset of MCI patients develop AD dementia [6,25], and there may be pathologic subtypes [26]. We also demonstrated DMN hyperconnectivity in MCI and ADMCI using network-level statistics. These changes may reflect both functional disconnection and compensation in response to damage at earlier stages of neurodegeneration, as well as direct or indirect pathologic mechanisms [27]. Moreover,

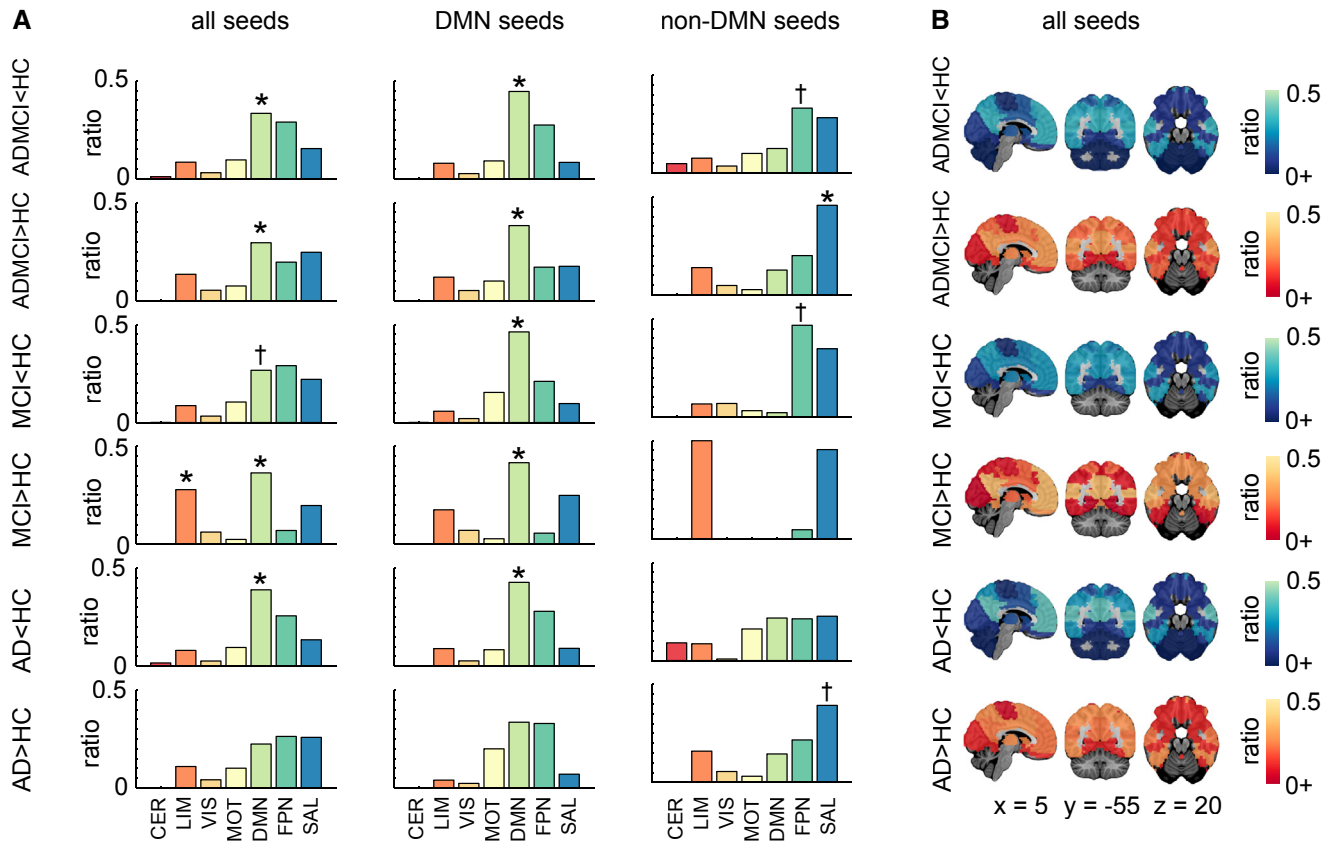


Fig. 3. Network-level findings using the R7 atlas. (A) Histograms showing per contrast the ratio of hits across the seven networks for all seeds, DMN seeds only, and non-DMN seeds. Networks with significant count (or hit) ratios are indicated by \* denoting  $qFDR < 0.05$ , whereas † denotes  $P < .05$  uncorrected. (B) Hit maps at R7 are shown for contrasts ADMCI < HC, ADMCI > HC, MCI < HC, MCI > HC, AD < HC, and AD > HC. Maps are superimposed onto the anatomic ICBM 152 template. x, y, and z MNI coordinates are given for sagittal, coronal, and axial slices. Abbreviations: AD, Alzheimer's disease dementia; ADMCI, AD dementia and MCI; CER, cerebellar network; DMN, default mode network; FDR, false discovery rate; FPN, frontoparietal network; HC, healthy control; LIM, limbic network; MCI, mild cognitive impairment; MOT, motor network; SAL, salience network; VIS, visual network.

there is some uncertainty of the specific nodes that actually show aberrant connectivity in our network-level analysis. This may give rise to apparent contradictory results.

#### 4.1.2. Early onset AD

DMN hypoconnectivity of similar magnitude to LOAD was demonstrated in early onset non-ADAD [28,29], whereas in ADAD, DMN hypoconnectivity was slightly more pronounced than that in LOAD [30]. Altered DMN connectivity was observed in asymptomatic mutation carriers (*PSEN1*, *PSEN2*, or *APP*) many years before the age at which they were expected to develop symptoms [31–33], suggesting that aberrant connectivity may be a very early biomarker for AD.

#### 4.1.3. Cognitively normal individuals at genetic risk for LOAD

Altered DMN connectivity has been reported in cognitively normal APOEε4 carriers compared with non-APOEε4 carriers. These alterations were found across all age groups, that is, elderly [12,34–36], middle-aged [37–39], and young

adults [40,41], and were associated with worse cognition in middle-aged and elderly carriers [35,37,39]. Studies have also reported connectivity changes in the DMN in the absence of Pittsburgh compound B–detectable brain amyloidosis [12,40,41], further validating the potential of rsfMRI connectivity as an early marker of synaptic and neuronal dysfunction in AD.

#### 4.1.4. Cognitively normal elderly at risk for LOAD

Aberrant DMN dysconnectivity, particularly reduced connectivity between the anterior and posterior DMN, has been associated with aging and age-related cognitive decline [33,42]. DMN hypoconnectivity may arise as early as middle age [43,44], with decreases occurring at differing rates between sexes [45] most likely due to the differential effect of sex on AD risk [46]. Reduced DMN integrity has also been reported in cognitively normal elderly with abnormal levels of CSF amyloid or tau proteins [47], as well as PET-detectable cerebral amyloidosis [48]. These results suggest that some of the effects related to normal aging in the literature may be driven by preclinical AD. Very few

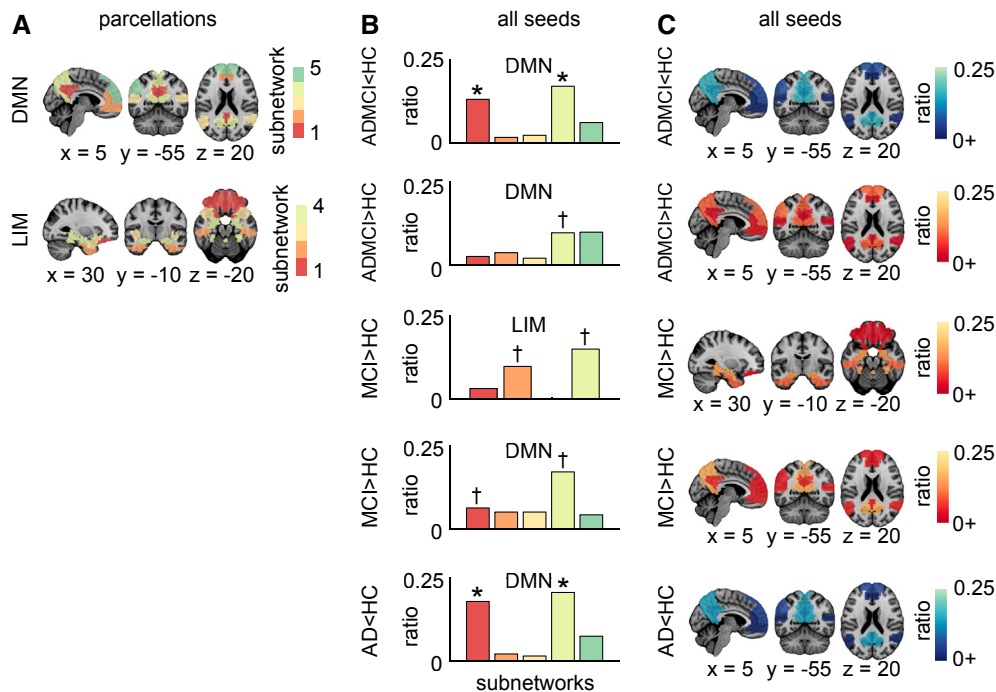


Fig. 4. Network-level findings using the R36 atlas. (A) Functional template at R36 showing the breakdown of the DMN and LIM into subnetworks. These two networks were significant ( $qFDR < 0.05$  for contrasts  $ADMCI < HC$  for DMN,  $ADMCI > HC$  for DMN,  $MCI > HC$  for DMN and LIM,  $AD < HC$  for DMN) or trended toward significance ( $P < .05$  uncorrected for contrasts  $MCI < HC$  for DMN) for the “all-seeds” condition at R7. (B) Histograms showing per selected contrast (as described in A), the ratio of counts (or hits) across the subnetworks. Subnetworks with significant hit ratios are indicated by \* denoting  $qFDR < 0.05$ , whereas  $^{\dagger}$  denotes a trend with  $P < .05$  uncorrected. (C) Hit maps at R36 for brain regions that overlap with significant or trending toward significance networks (as described in A). Maps are superimposed onto the anatomic ICBM 152 template. x, y, and z MNI coordinates are given for sagittal, coronal, and axial slices. Abbreviations: AD, Alzheimer's disease dementia; ADMCI, AD dementia and MCI; CER, cerebellar network; DMN, default mode network; FDR, false discovery rate; FPN, frontoparietal network; HC, healthy control; LIM, limbic network; MCI, mild cognitive impairment; MOT, motor network; SAL, salience network; VIS, visual network.

studies examined the interactions between age, sex, LOAD, and rsfMRI connectivity, which is clearly an important avenue for future work.

#### 4.2. Connectivity changes outside the DMN

Our meta-analysis confirmed that intrinsic connectivity disruptions in LOAD are not confined to the DMN. We found increased connectivity in the SAL in ADMCI and AD. Abnormal SAL connectivity has now been reported in another LOAD study [49] published after we completed our meta-analysis and has also been demonstrated in ADAD [30], APOE $\epsilon$ 4 carriers [36,37], and the elderly [50], with connectivity increases highlighted in APOE $\epsilon$ 4 carriers. With the anterior insula as a key hub, the SAL plays a pivotal role in network switching between the DMN and frontoparietal network (FPN), two networks exhibiting competitive interactions during cognitive information processing [51]. Association of heightened SAL connectivity with reduced DMN connectivity in AD suggests that progressive DMN impairment may be deleterious to SAL function [52].

We also found increased connectivity in the LIM in MCI. Heightened LIM connectivity has been reported in

early onset, non-ADAD patients [29], and in individuals with subjective memory impairment [53]. The effect of APOE $\epsilon$ 4 carriage on LIM connectivity, however, lacks consensus [54–56]. Since LIM hyperconnectivity in early onset AD patients was shown to correlate positively with memory performance, it is likely that increased connectivity in this network contributes to preserving function in the face of medial temporal lobe pathology [29].

#### 4.3. Selective vulnerability of multimodal networks in AD

The DMN, SAL, and FPN are multimodal networks that interconnect cortical regions associated with various cognitive functions, and they have been demonstrated computationally to support integrative information processing at the cost of being vulnerable to early and fast spreading of insults [57]. Supporting this theoretical finding is the recent observation that tau and amyloid- $\beta$ , despite their independent patterns of spatial deposition, overlap with brain tissue loss in hub regions of multimodal networks [58]. These multimodal networks are also metabolically expensive and display higher rates of cerebral blood flow, aerobic glycolysis, and oxidative

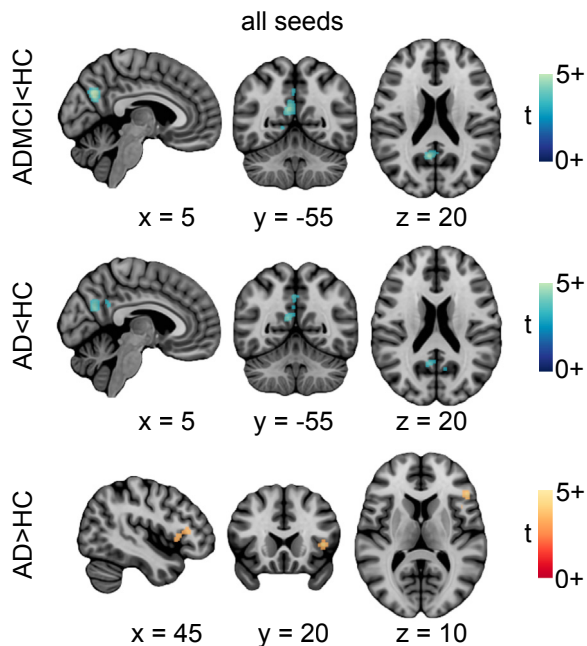


Fig. 5. Location of significant convergence of the voxel-level findings. Regions exhibiting significant rsfMRI abnormalities for contrasts ADMCI < HC, AD < HC, and AD > HC. Activation likelihood estimation images were thresholded at  $P < .05$  (cluster-level family wise error or FWE corrected for multiple comparisons; cluster-forming threshold  $P < .001$  at the voxel level) and displayed as  $t$  scores, with hyperconnectivity in red-orange and hypoconnectivity in blue-green. Maps are superimposed onto the anatomic ICBM 152 template.  $x$ ,  $y$ , and  $z$  MNI coordinates are given for sagittal, coronal, and axial slices. Abbreviations: AD, Alzheimer's disease dementia; ADMCI, AD dementia and mild cognitive impairment; HC, healthy control; rsfMRI, resting-state functional magnetic resonance imaging.

glucose metabolism [59]. The high-value/high-cost characteristics of the DMN, SAL, and FPN may make them vulnerable to AD-associated pathogenic processes, such as metabolic dysfunction/oxidative stress, and accumulation of toxic proteins, such as amyloid- $\beta$  [59]. The hypothesis that multimodal networks/regions are particularly susceptible to AD-associated pathophysiological processes may explain our finding of consistent alterations of these networks.

#### 4.4. Limitations

Our literature search did not identify an abundance of rsfMRI literature in AD and MCI cohorts, which clearly expresses the need for additional research. The relatively low number of experiments that met our inclusion criteria might have underpowered our voxel-level findings, especially for the MCI contrasts. In addition, our search demonstrated that typical studies featured small samples, and also that analytical methods were quite variable in the field (a main reason for excluding an article was due to methodology used). This setting is particularly amenable to questionable research practices, including

“p-hacking” (testing several methods, reporting only one). Given the near absence of negative results reporting in the field, on one hand, and the large size of the rsfMRI field, on the other hand, there is no question that some amount of publication bias is also present. Meta-analytical tools, such as funnel plots, are available to detect both selective reporting and p-hacking but are not feasible given current reporting practices in the rsfMRI community [60].

Another limitation of our study is experimental heterogeneity, in terms of population recruitment, scan acquisition (e.g., scanner make and model, scanning parameters), and processing choices [13,20,61]. The prominence of the DMN in our results partly reflects the focus on this network in the literature, which we quantified using seed statistics. Hypothesis-driven analyses on the DMN are attractive for assessing connectivity changes in small samples; as such analyses will have good statistical power if the DMN truly carries the larger effects in the brain. However, full-brain studies will be required to get a more comprehensive view on AD-related changes in rsfMRI network connectivity using meta-analyses. The current trend toward large public samples [13,62] is enabling unbiased meta-analyses, pooling neuroimaging data across many studies instead of relying on published coordinates. This will hopefully resolve most of the aforementioned limitations in the future.

## 5. Conclusions

Our meta-analysis demonstrated consistent connectivity alterations in the DMN, SAL, and LIM in the spectrum of LOAD, supporting the use of resting-state connectivity as a biomarker of AD.

## Acknowledgments

The computational resources used to perform the data analysis were provided by Compute Canada ([www.computeCanada.org](http://www.computeCanada.org)) and CLUMEQ ([www.clumeq.mcgill.ca](http://www.clumeq.mcgill.ca)), which is funded in part by NSERC (MRS), FQRNT, and McGill University.

This research was supported by the Canadian Consortium on Neurodegeneration in Aging. The Canadian Consortium on Neurodegeneration in Aging is supported by a grant from the Canadian Institutes of Health Research with funding from several partners including the Alzheimer Society of Canada, Sanofi, and Women's Brain Health Initiative. This research was also supported by the Courtois Foundation (P.B.) and an Alzheimer Society Postdoctoral Fellowship (A.B.).

## Supplementary data

Supplementary data related to this article can be found at <http://dx.doi.org/10.1016/j.dadm.2017.03.007>.

## RESEARCH IN CONTEXT

1. Systematic review: We conducted a systematic review of PubMed-indexed resting-state functional magnetic resonance imaging (rsfMRI) studies in accordance with the “Preferred Reporting Items for Systematic Reviews and Meta-Analyses” guidelines. We included studies that investigated differences in functional connectivity, relative to controls, between patients with Alzheimer’s disease (AD) and/or mild cognitive impairment, and reported coordinates of findings.
2. Interpretation: Typical rsfMRI functional connectivity studies in AD suffer from low statistical power. Our meta-analysis quantifies if and where convergent findings have been reported in the literature and strengthens the evidence for the use of rsfMRI as an AD biomarker.
3. Future directions: A disproportionately large portion of studies specifically investigated the default mode network, based on well-grounded hypotheses on AD pathophysiology. It is unclear if AD truly has larger effects on default-mode connectivity because of limited power to examine other networks. Future research should aim for full-brain investigations using larger study populations.

## References

- [1] Sperling RA, Aisen PS, Beckett LA, Bennett DA, Craft S, Fagan AM, et al. Toward defining the preclinical stages of Alzheimer’s disease: recommendations from the National Institute on Aging–Alzheimer’s Association workgroups on diagnostic guidelines for Alzheimer’s disease. *Alzheimers Dement* 2011; 7:280–92.
- [2] Wu L, Rosa-Neto P, Hsiung GY, Sadovnick AD, Masellis M, Black SE, et al. Early-onset familial Alzheimer’s disease (EOFAD). *Can J Neurol Sci* 2012;39:436–45.
- [3] Campion D, Dumanchin C, Hannequin D, Dubois B, Belliard S, Puel M, et al. Early-onset autosomal dominant Alzheimer disease: prevalence, genetic heterogeneity, and mutation spectrum. *Am J Hum Genet* 1999;65:664–70.
- [4] Hughes RE, Nikolic K, Ramsay RR. One for all? Hitting multiple Alzheimer’s disease targets with one drug. *Front Neurosci* 2016;10:177.
- [5] Matthews PM, Hampshire A. Clinical concepts emerging from fMRI functional connectomics. *Neuron* 2016;91:511–28.
- [6] Albert MS, DeKosky ST, Dickson D, Dubois B, Feldman HH, Fox NC, et al. The diagnosis of mild cognitive impairment due to Alzheimer’s disease: recommendations from the National Institute on Aging–Alzheimer’s Association workgroups on diagnostic guidelines for Alzheimer’s disease. *Alzheimers Dement* 2011; 7:270–9.
- [7] Vemuri P, Jones DT, Jack CR Jr. Resting state functional MRI in Alzheimer’s disease. *Alzheimers Res Ther* 2012;4:2.
- [8] Logothetis NK. The neural basis of the blood-oxygen-level-dependent functional magnetic resonance imaging signal. *Philos Trans R Soc Lond B Biol Sci* 2002;357:1003–37.
- [9] Krajcovicova L, Marecek R, Mikl M, Rektorova I. Disruption of resting functional connectivity in Alzheimer’s patients and at-risk subjects. *Curr Neurol Neurosci Rep* 2014;14:491.
- [10] Brier MR, Thomas JB, Ances BM. Network dysfunction in Alzheimer’s disease: refining the disconnection hypothesis. *Brain Connect* 2014;4:299–311.
- [11] Jack CR Jr, Knopman DS, Jagust WJ, Petersen RC, Weiner MW, Aisen PS, et al. Tracking pathophysiological processes in Alzheimer’s disease: an updated hypothetical model of dynamic biomarkers. *Lancet Neurol* 2013;12:207–16.
- [12] Sheline YI, Morris JC, Snyder AZ, Price JL, Yan Z, D’Angelo G, et al. APOE4 allele disrupts resting state fMRI connectivity in the absence of amyloid plaques or decreased CSF Aβ42. *J Neurosci* 2010; 30:17035–40.
- [13] Tam A, Dansereau C, Badhwar A, Orban P, Belleville S, Chertkow H, et al. Common effects of amnesic mild cognitive impairment on resting-state connectivity across four independent studies. *Front Aging Neurosci* 2015;7:242.
- [14] Moher D, Liberati A, Tetzlaff J, Altman DG, PRISMA Group. Preferred reporting items for systematic reviews and meta-analyses: the PRISMA statement. *Int J Surg* 2010;8:336–41.
- [15] Bellec P, Benhajali Y, Carbonell F, Dansereau C, Albouy G, Pelland M, et al. Impact of the resolution of brain parcels on connectome-wide association studies in fMRI. *Neuroimage* 2015;123:212–28.
- [16] Lancaster JL, Tordesillas-Gutiérrez D, Martinez M, Salinas F, Evans A, Zilles K, et al. Bias between MNI and Talairach coordinates analyzed using the ICBM-152 brain template. *Hum Brain Mapp* 2007; 28:1194–205.
- [17] Phipson B, Smyth GK. Permutation P-values should never be zero: calculating exact P-values when permutations are randomly drawn. *Stat Appl Genet Mol Biol* 2010;9. Article39.
- [18] Benjamini Y, Hochberg Y. Controlling the false discovery rate: a practical and powerful approach to multiple testing. *J R Stat Soc Ser B Stat Methodol* 1995;57:289–300.
- [19] Eickhoff SB, Bzdok D, Laird AR, Kurth F, Fox PT. Activation likelihood estimation meta-analysis revisited. *Neuroimage* 2012; 59:2349–61.
- [20] Eickhoff SB, Nichols TE, Laird AR, Hoffstaedter F, Amunts K, Fox PT, et al. Behavior, sensitivity, and power of activation likelihood estimation characterized by massive empirical simulation. *Neuroimage* 2016;137:70–85.
- [21] Li HJ, Hou XH, Liu HH, Yue CL, He Y, Zuo XN. Toward systems neuroscience in mild cognitive impairment and Alzheimer’s disease: a meta-analysis of 75 fMRI studies. *Hum Brain Mapp* 2015; 36:1217–32.
- [22] Jacobs HIL, Radua J, Lückmann HC, Sack AT. Meta-analysis of functional network alterations in Alzheimer’s disease: toward a network biomarker. *Neurosci Biobehav Rev* 2013;37:753–65.
- [23] Kim HJ, Cha J, Lee JM, Shin JS, Jung NY, Kim YJ, et al. Distinctive resting state network disruptions among Alzheimer’s disease, subcortical vascular dementia, and mixed dementia patients. *J Alzheimers Dis* 2016;50:709–18.
- [24] Buckner RL, Sepulcre J, Talukdar T, Krienen FM, Liu H, Hedden T, et al. Cortical hubs revealed by intrinsic functional connectivity: mapping, assessment of stability, and relation to Alzheimer’s disease. *J Neurosci* 2009;29:1860–73.
- [25] Malek-Ahmadi M. Reversion from mild cognitive impairment to normal cognition: a meta-analysis. *Alzheimer Dis Assoc Disord* 2016;30:324–30.
- [26] Köhler S, Hamel R, Sijm M, Koene T, Pijnenburg YAL, van der Flier WM, et al. Progression to dementia in memory clinic patients without dementia: a latent profile analysis. *Neurology* 2013;81:1342–9.
- [27] Jones DT, Knopman DS, Gunter JL, Graff-Radford J, Vemuri P, Boeve BF, et al. Cascading network failure across the Alzheimer’s disease spectrum. *Brain* 2016;139:547–62.
- [28] Adriaanse SM, Binnewijzend MA, Ossenkoppele R, Tijms BM, van der Flier WM, Koene T, et al. Widespread disruption of functional

- brain organization in early-onset Alzheimer's disease. *PLoS One* 2014;9:e102995.
- [29] Gour N, Felician O, Didic M, Koric L, Gueriot C, Chanoine V, et al. Functional connectivity changes differ in early and late-onset Alzheimer's disease. *Hum Brain Mapp* 2014;35:2978–94.
- [30] Thomas JB, Brier MR, Bateman RJ, Snyder AZ, Benzinger TL, Xiong C, et al. Functional connectivity in autosomal dominant and late-onset Alzheimer disease. *JAMA Neurol* 2014;71:1111–22.
- [31] Quiroz YT, Schultz AP, Chen K, Protas HD, Brickhouse M, Fleisher AS, et al. Brain imaging and blood biomarker abnormalities in children with autosomal dominant Alzheimer disease: a cross-sectional study. *JAMA Neurol* 2015;72:912–9.
- [32] Chhatwal JP, Schultz AP, Johnson K, Benzinger TL, Jack C Jr, Ances BM, et al. Impaired default network functional connectivity in autosomal dominant Alzheimer disease. *Neurology* 2013;81:736–44.
- [33] Sala-Llloch R, Fortea J, Bartrés-Faz D, Bosch B, Lladó A, Peña-Gómez C, et al. Evolving brain functional abnormalities in PSEN1 mutation carriers: a resting and visual encoding fMRI study. *J Alzheimers Dis* 2013;36:165–75.
- [34] Shu H, Shi Y, Chen G, Wang Z, Liu D, Yue C, et al. Opposite neural trajectories of apolipoprotein E  $\epsilon$ 4 and  $\epsilon$ 2 alleles with aging associated with different risks of Alzheimer's disease. *Cereb Cortex* 2016;26:1421–9.
- [35] Song H, Long H, Zuo X, Yu C, Liu B, Wang Z, et al. APOE effects on default mode network in Chinese cognitive normal elderly: relationship with clinical cognitive performance. *PLoS One* 2015;10:e0133179.
- [36] Machulda MM, Jones DT, Vemuri P, McDade E, Avula R, Przybelski S, et al. Effect of APOE  $\epsilon$ 4 status on intrinsic network connectivity in cognitively normal elderly subjects. *Arch Neurol* 2011;68:1131–6.
- [37] Goveas JS, Xie C, Chen G, Li W, Ward BD, Franczak MB, et al. Functional network endophenotypes unravel the effects of apolipoprotein E epsilon 4 in middle-aged adults. *PLoS One* 2013;8:e55902.
- [38] Patel KT, Stevens MC, Pearlson GD, Winkler AM, Hawkins KA, Skudlarski P, et al. Default mode network activity and white matter integrity in healthy middle-aged ApoE4 carriers. *Brain Imaging Behav* 2013;7:60–7.
- [39] Westlye ET, Lundervold A, Rootwelt H, Lundervold AJ, Westlye LT. Increased hippocampal default mode synchronization during rest in middle-aged and elderly APOE  $\epsilon$ 4 carriers: relationships with memory performance. *J Neurosci* 2011;31:7775–83.
- [40] Su YY, Liang X, Schoepf UJ, Varga-Szemes A, West HC, Qi R, et al. APOE polymorphism affects brain default mode network in healthy young adults: a STROBE article. *Medicine* 2015;94:e1734.
- [41] Filippini N, MacIntosh BJ, Hough MG, Goodwin GM, Frisoni GB, Smith SM, et al. Distinct patterns of brain activity in young carriers of the APOE-epsilon4 allele. *Proc Natl Acad Sci U S A* 2009;106:7209–14.
- [42] Ferreira LK, Busatto GF. Resting-state functional connectivity in normal brain aging. *Neurosci Biobehav Rev* 2013;37:384–400.
- [43] Evers EA, Klaassen EB, Rombouts SA, Backes WH, Jolles J. The effects of sustained cognitive task performance on subsequent resting state functional connectivity in healthy young and middle-aged male school teachers. *Brain Connect* 2012;2:102–12.
- [44] Zuo XN, Kelly C, Di Martino A, Mennes M, Margulies DS, Bangaru S, et al. Growing together and growing apart: regional and sex differences in the lifespan developmental trajectories of functional homotopy. *J Neurosci* 2010;30:15034–43.
- [45] Scheinost D, Finn ES, Tokoglu F, Shen X, Papademetris X, Hampson M, et al. Sex differences in normal age trajectories of functional brain networks. *Hum Brain Mapp* 2015;36:1524–35.
- [46] Podcasy JL, Epperson CN. Considering sex and gender in Alzheimer disease and other dementias. *Dialogues Clin Neurosci* 2016;18:437–46.
- [47] Wang L, Brier MR, Snyder AZ, Thomas JB, Fagan AM, Xiong C, et al. Cerebrospinal fluid A $\beta$ 42, phosphorylated Tau181, and resting-state functional connectivity. *JAMA Neurol* 2013;70:1242–8.
- [48] Elman JA, Madison CM, Baker SL, Vogel JW, Marks SM, Crowley S, et al. Effects of beta-amyloid on resting state functional connectivity within and between networks reflect known patterns of regional vulnerability. *Cereb Cortex* 2016;26:695–707.
- [49] Wang Z, Zhang M, Han Y, Song H, Guo R, Li K. Differentially disrupted functional connectivity of the subregions of the amygdala in Alzheimer's disease. *J Xray Sci Technol* 2016;24:329–42.
- [50] Sala-Llloch R, Bartrés-Faz D, Junqué C. Reorganization of brain networks in aging: a review of functional connectivity studies. *Front Psychol* 2015;6:663.
- [51] He X, Qin W, Liu Y, Zhang X, Duan Y, Song J, et al. Abnormal salience network in normal aging and in amnesic mild cognitive impairment and Alzheimer's disease. *Hum Brain Mapp* 2014;35:3446–64.
- [52] Zhou J, Greicius MD, Gennatas ED, Growdon ME, Jang JY, Rabinovici GD, et al. Divergent network connectivity changes in behavioural variant frontotemporal dementia and Alzheimer's disease. *Brain* 2010;133:1352–67.
- [53] Gour N, Ranjeva JP, Ceccaldi M, Confort-Gouny S, Barbeau E, Soulier E, et al. Basal functional connectivity within the anterior temporal network is associated with performance on declarative memory tasks. *Neuroimage* 2011;58:687–97.
- [54] Heise V, Filippini N, Trachtenberg AJ, Suri S, Ebmeier KP, Mackay CE. Apolipoprotein E genotype, gender and age modulate connectivity of the hippocampus in healthy adults. *Neuroimage* 2014;98:23–30.
- [55] Matura S, Prvulovic D, Butz M, Hartmann D, Sepanski B, Linnemann K, et al. Recognition memory is associated with altered resting-state functional connectivity in people at genetic risk for Alzheimer's disease. *Eur J Neurosci* 2014;40:3128–35.
- [56] Trachtenberg AJ, Filippini N, Ebmeier KP, Smith SM, Karpe F, Mackay CE. The effects of APOE on the functional architecture of the resting brain. *Neuroimage* 2012;59:565–72.
- [57] Misić B, Betzel RF, Nematzadeh A, Goñi J, Griffa A, Hagmann P, et al. Cooperative and competitive spreading dynamics on the human connectome. *Neuron* 2015;86:1518–29.
- [58] Sepulcre J, Schultz AP, Sabuncu M, Gomez-Isla T, Chhatwal J, Becker A, et al. In vivo tau, amyloid, and gray matter profiles in the aging brain. *J Neurosci* 2016;36:7364–74.
- [59] Crossley NA, Mechelli A, Scott J, Carletti F, Fox PT, McGuire P, et al. The hubs of the human connectome are generally implicated in the anatomy of brain disorders. *Brain* 2014;137:2382–95.
- [60] Sterne JA, Egger M. Funnel plots for detecting bias in meta-analysis: guidelines on choice of axis. *J Clin Epidemiol* 2001;54:1046–55.
- [61] Jones DT, Vemuri P, Murphy MC, Gunter JL, Senjem ML, Machulda MM, et al. Non-stationarity in the “resting brain's” modular architecture. *PLoS One* 2012;7:e39731.
- [62] Cheng W, Palaniyappan L, Li M, Kendrick KM, Zhang J, Luo Q, et al. Voxel-based, brain-wide association study of aberrant functional connectivity in schizophrenia implicates thalamocortical circuitry. *NPJ Schizophr* 2015;1:15016.
- [63] Wang K, Liang M, Wang L, Tian L, Zhang X, Li K, et al. Altered functional connectivity in early Alzheimer's disease: a resting-state fMRI study. *Hum Brain Mapp* 2007;28:967–78.
- [64] Zhang H-Y, Wang S-J, Xing J, Liu B, Ma Z-L, Yang M, et al. Detection of PCC functional connectivity characteristics in resting-state fMRI in mild Alzheimer's disease. *Behav Brain Res* 2009;197:103–8.
- [65] Zhang H-Y, Wang S-J, Liu B, Ma Z-L, Yang M, Zhang Z-J, et al. Resting brain connectivity: changes during the progress of Alzheimer disease. *Radiology* 2010;256:598–606.
- [66] Sheline YI, Raichle ME, Snyder AZ, Morris JC, Head D, Wang S, et al. Amyloid plaques disrupt resting state default mode network connectivity in cognitively normal elderly. *Biol Psychiatry* 2010;67:584–7.

- [67] Gili T, Cercignani M, Serra L, Perri R, Giove F, Maraviglia B, et al. Regional brain atrophy and functional disconnection across Alzheimer's disease evolution. *J Neurol Neurosurg Psychiatry* 2011;82:58–66.
- [68] Wu X, Li R, Fleisher AS, Reiman EM, Guan X, Zhang Y, et al. Altered default mode network connectivity in Alzheimer's disease—a resting functional MRI and Bayesian network study. *Hum Brain Mapp* 2011;32:1868–81.
- [69] Li R, Wu X, Fleisher AS, Reiman EM, Chen K, Yao L. Attention-related networks in Alzheimer's disease: a resting functional MRI study. *Hum Brain Mapp* 2012;33:1076–88.
- [70] Damoiseaux JS, Prater KE, Miller BL, Greicius MD. Functional connectivity tracks clinical deterioration in Alzheimer's disease. *Neurobiol Aging* 2012;33:828.e19–30.
- [71] Binnewijzend MAA, Schoonheim MM, Sanz-Arigita E, Wink AM, van der Flier WM, Tolboom N, et al. Resting-state fMRI changes in Alzheimer's disease and mild cognitive impairment. *Neurobiol Aging* 2012;33:2018–28.
- [72] Kenny ER, Blamire AM, Firbank MJ, O'Brien JT. Functional connectivity in cortical regions in dementia with Lewy bodies and Alzheimer's disease. *Brain* 2012;135:569–81.
- [73] Zhu DC, Majumdar S, Korolev IO, Berger KL, Bozoki AC. Alzheimer's disease and amnesic mild cognitive impairment weaken connections within the default-mode network: a multi-modal imaging study. *J Alzheimers Dis* 2013;34:969–84.
- [74] Balthazar MLF, Pereira FRS, Lopes TM, da Silva EL, Coan AC, Campos BM, et al. Neuropsychiatric symptoms in Alzheimer's disease are related to functional connectivity alterations in the salience network. *Hum Brain Mapp* 2014;35:1237–46.
- [75] Yao H, Liu Y, Zhou B, Zhang Z, An N, Wang P, et al. Decreased functional connectivity of the amygdala in Alzheimer's disease revealed by resting-state fMRI. *Eur J Radiol* 2013;82:1531–8.
- [76] Zhou B, Liu Y, Zhang Z, An N, Yao H, Wang P, et al. Impaired functional connectivity of the thalamus in Alzheimer's disease and mild cognitive impairment: a resting-state fMRI study. *Curr Alzheimer Res* 2013;10:754–66.
- [77] Zhang Z, Liu Y, Zhou B, Zheng J, Yao H, An N, et al. Altered functional connectivity of the marginal division in Alzheimer's disease. *Curr Alzheimer Res* 2014;11:145–55.
- [78] Weiler M, Fukuda A, Massabki LHP, Lopes TM, Franco AR, Damasceno BP, et al. Default mode, executive function, and language functional connectivity networks are compromised in mild Alzheimer's disease. *Curr Alzheimer Res* 2014;11:274–82.
- [79] Balachandar R, John JP, Saini J, Kumar KJ, Joshi H, Sadanand S, et al. A study of structural and functional connectivity in early Alzheimer's disease using rest fMRI and diffusion tensor imaging. *Int J Geriatr Psychiatry* 2015;30:497–504.
- [80] Pasquini L, Scherr M, Tahmasian M, Meng C, Myers NE, Ortner M, et al. Link between hippocampus' raised local and eased global intrinsic connectivity in AD. *Alzheimers Dement* 2015;11:475–84.
- [81] Yi D, Choe YM, Byun MS, Sohn BK, Seo EH, Han J, et al. Differences in functional brain connectivity alterations associated with cerebral amyloid deposition in amnesic mild cognitive impairment. *Front Aging Neurosci* 2015;7:15.
- [82] Sorg C, Riedl V, Mühlau M, Calhoun VD, Eichele T, Läer L, et al. Selective changes of resting-state networks in individuals at risk for Alzheimer's disease. *Proc Natl Acad Sci U S A* 2007;104:18760–5.
- [83] Bai F, Watson DR, Yu H, Shi Y, Yuan Y, Zhang Z. Abnormal resting-state functional connectivity of posterior cingulate cortex in amnesic type mild cognitive impairment. *Brain Res* 2009;1302:167–74.
- [84] Bai F, Watson DR, Shi Y, Wang Y, Yue C, YuhuanTeng, et al. Specifically Progressive Deficits of Brain Functional Marker in Amnesic Type Mild Cognitive Impairment. *PLoS One* 2011;6:e24271.
- [85] Xie C, Bai F, Yuan B, Yu H, Shi Y, Yuan Y, et al. Joint effects of gray matter atrophy and altered functional connectivity on cognitive deficits in amnesic mild cognitive impairment patients. *Psychol Med* 2015;45:1799–810.
- [86] Jin M, Pelak VS, Cordes D. Aberrant default mode network in subjects with amnesic mild cognitive impairment using resting-state functional MRI. *Magn Reson Imaging* 2012;30:48–61.
- [87] Han SD, Arfanakis K, Fleischman DA, Leurgans SE, Tuminello ER, Edmonds EC, et al. Functional connectivity variations in mild cognitive impairment: associations with cognitive function. *J Int Neuropsychol Soc* 2012;18:39–48.
- [88] Liang P, Wang Z, Yang Y, Li K. Three subsystems of the inferior parietal cortex are differently affected in mild cognitive impairment. *J Alzheimers Dis* 2012;30:475–87.
- [89] Hahn K, Myers N, Prigarin S, Rodenacker K, Kurz A, Förstl H, et al. Selectively and progressively disrupted structural connectivity of functional brain networks in Alzheimer's disease - revealed by a novel framework to analyze edge distributions of networks detecting disruptions with strong statistical evidence. *Neuroimage* 2013;81:96–109.
- [90] Myers N, Pasquini L, Götter J, Grimmer T, Koch K, Ortner M, et al. Within-patient correspondence of amyloid- $\beta$  and intrinsic network connectivity in Alzheimer's disease. *Brain* 2014;137:2052–64.
- [91] Koch K, Myers NE, Götter J, Pasquini L, Grimmer T, Förster S, et al. Disrupted Intrinsic Networks Link Amyloid- $\beta$  Pathology and Impaired Cognition in Prodromal Alzheimer's Disease. *Cereb Cortex* 2015;25:4678–88.
- [92] Das SR, Pluta J, Mancuso L, Kliot D, Yushkevich PA, Wolk DA. Anterior and posterior MTL networks in aging and MCI. *Neurobiol Aging* 2015;36 Suppl 1:S141–50.e1.
- [93] Gardini S, Venneri A, Sambataro F, Cuetos F, Fasano F, Marchi M, et al. Increased functional connectivity in the default mode network in mild cognitive impairment: a maladaptive compensatory mechanism associated with poor semantic memory performance. *J Alzheimers Dis* 2015;45:457–70.